Search for di-Higgs production with the ATLAS detector

Maosen Zhou, on behalf of the ATLAS collaboration

Institute of High Energy Physics, CAS

maosen.zhou@cern.ch

1 Introduction

The SM production of Higgs boson pairs (hh), as shown in Figure 1(a) and Figure 1(b), is not expected to be observable using the datasets so far recorded by the ATLAS experiment, because of the small cross-section (33.41 fb). However, a variety of new physics models predict enhancements to this cross-section. Therefore, the observation of Higgs boson pairs would provide supporting evidence for BSM physics. Models with two Higgs doublets (2HDMs), such as the minimal supersymmetric extension of the SM, twin Higgs models and composite Higgs models, predict the existence of a heavy Higgs boson that could itself decay to two lighter, SM-like, scalar partners, as shown in Figure 1(c). Other BSM resonances such as gravitons, radions or stoponium could also decay into Higgs boson pairs. Finally, a deviation from the SM value of the self-coupling λ_{hhh}, or new EFT-like couplings (for example, direct $tt\bar{h}h$ vertices) could increase the non-resonant production rate.

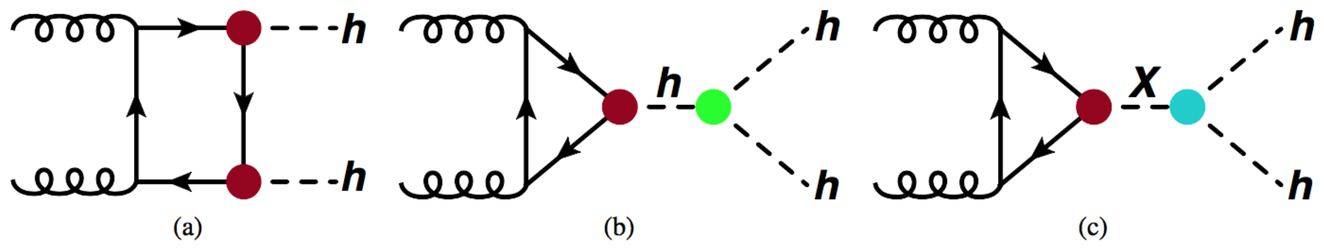

Figure 1: The Feyman diagrams for leading-order non-resonant hh production ((a), (b)) and resonant hh production ((c)).

2 Overview on different search channels

Since Run 1, ATLAS has published the results of searches in the following channels:

- $\boldsymbol{hh \to b\bar{b}\gamma\gamma}$: this final state benefits from the large branching fraction of the $h \to b\bar{b}$ decay (58%) and the clean diphoton signal, due to high $m_{\gamma\gamma}$ resolution and strong jet rejection.
- $\boldsymbol{hh \to b\bar{b}b\bar{b}}$: it makes use of the dominant $h \to b\bar{b}$ decay mode.
- $\boldsymbol{hh \to WW^*(\to \ell\nu q\bar{q})\gamma\gamma}$: this final state benefits from a large branching fraction from $h \to WW^*$, a clean signature from two photons and one lepton.
- $\boldsymbol{hh \to bb\tau\tau(\to e/\mu\tau_{\text{had}})}$: this channel has the third largest branching fraction (7.4%) and is relatively clean compared to the channels with larger branching fractions.

	bb	WW	ττ	ZZ	γγ
bb	33%				
WW	25%	4.6%			
ττ	7.4%	2.5%	0.39%		
ZZ	3.1%	1.2%	0.34%	0.076%	
γγ	0.26%	0.10%	0.029%	0.013%	0.0053%

Figure 2: The different decay modes of the di-Higgs system and corresponding relative branching fractions.

3 The Run 1 combination

In Run 1, no significant excess is observed, combining four channels. For the resonant results, the improvement above m_H=500 GeV is due to the sensitivity of the $hh \to b\bar{b}b\bar{b}$ analysis. In this poster, all the limits are obtained assuming SM values for the h decay branching ratios, and the resonance with narrow width (10 MeV) is assumed.

Expected	100	680	130	63	48
Observed	220	1150	160	63	70

Table 1: The expected and observed 95% CL upper limits on the cross sections of non-resonant hh production relative to the SM prediction at $\sqrt{s}$ =8 TeV from individual analyses and their combinations. The cross-section of SM Higgs pair production is 9.9±1.3 fb with m_h=125.4 GeV, calculated at NNLO.

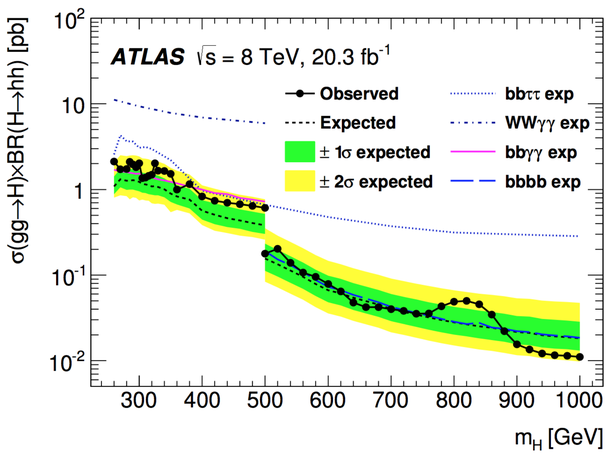

Figure 3: The observed and expected 95% CL upper limits on resonant hh production at $\sqrt{s}$ =8 TeV as functions of the heavy Higgs boson mass m_H. The expected limits from individual analyses are also shown.

4 $hh \to b\bar{b}\gamma\gamma$

- Two isolated photons, $p_T^{\gamma 1}(p_T^{\gamma 2})/m_{\gamma\gamma}$ >0.35(0.25);
- Two $b-$jets (85% $b-$tagging efficiency), $p_T^{b1}(p_T^{b2})$ >55(35) GeV;
- m_h/m_{bb} scaling to improve $m_{bb\gamma\gamma}$ resolution;
- $|m_{\gamma\gamma} - m_h| < 2\sigma_{\gamma\gamma}$, where $\sigma_{\gamma\gamma}$=1.55 GeV;
- $m_{bb\gamma\gamma}$ mass window containing 95% of resonant signal events (based on signal simulation).

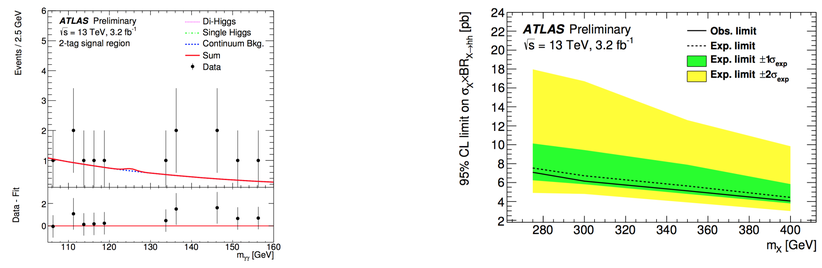

Figure 4: Left: the distribution of $m_{\gamma\gamma}$ in signal region for non-resonant search, corresponding to 117 times SM prediction; right: the observed (expected) limits for resonant search.

5 $hh \to b\bar{b}b\bar{b}$

Resolved

300 GeV$\leq m_H <$1200 GeV, including non-resonant search.

- Four $anti-k_T$ jets with R=0.4;
- Four $b-$jets (70% $b-$tagging efficiency);
- m_{4j} dependent p_T cut of Higgs candidate;
- $|\Delta\eta_{hh}| <\sim$1.1 (m_{4j} dependent).

Boosted

$m_H >$1000 GeV

- Two $anti-k_T$ jets with R=1;
- Each large-R jets has at least one associated small-R $b-$tagged track jet;
- $p_T^{J1}(p_T^{J2})$ >450 (250) Gev;
- $|\Delta\eta_{hh}| <$1.7

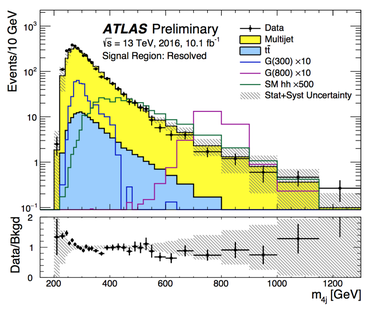

Figure 5: The distribution of m_{4j} in signal region for resolved analysis.

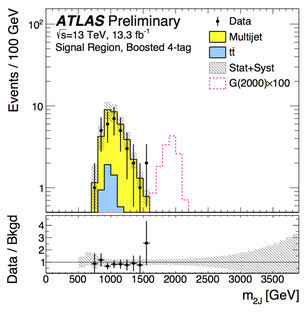

Figure 6: The distribution of m_{2J} in signal region for boosted analysis.

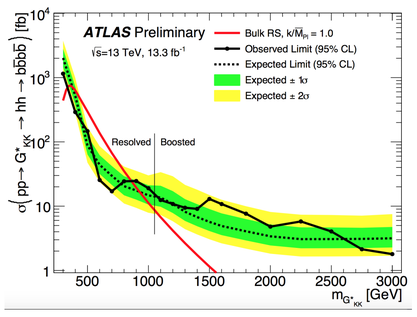

Figure 7: The observed (expected) limits for resonant search. The non-resonant limit corresponds to 29 times SM prediction.

6 $hh \to WW^*\gamma\gamma$

- Two well isolatd and identified photons, $p_T^{\gamma 1}(p_T^{\gamma 2})/m_{\gamma\gamma}$ >0.35(0.25);
- At least two central jets ($|\eta| <$2.5);
- $b-$veto;
- At least one lepton;
- $|m_{\gamma\gamma} - 125.09| < 2\sigma_{\gamma\gamma}$, where $\sigma_{\gamma\gamma}$=1.7 GeV;

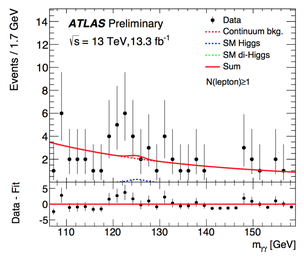

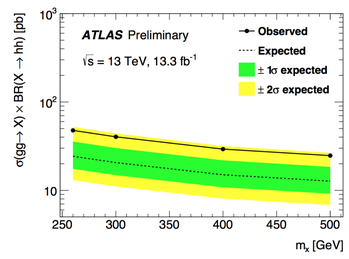

Figure 8: Left: the distribution of $m_{\gamma\gamma}$ in signal region; right: the observed (expected) limits for resonant search. The non-resonant limit corresponds to 749 times SM prediction.

7 Summary

This poster summarizes the search for both non-resonant and resonant Higgs boson pair production in Run 1 and latest results in Run 2 with the ATLAS detector at LHC. The search is performed in $hh \to b\bar{b}\gamma\gamma$, $hh \to b\bar{b}b\bar{b}$, $hh \to WW^*\gamma\gamma$, $hh \to b\bar{b}\tau\tau$ final states. No significant excess is observed in the data beyond the background expectation. The best upper limit on the hh production cross section has been achieved by $hh \to b\bar{b}b\bar{b}$ in Run 2. For the non-resonant hh production, the observed limit relative to the SM prediction changes from 70 in Run 1, combining four channels, to 30 in Run 2, which is obtained from single $hh \to b\bar{b}b\bar{b}$ channel; for the resonant production, comparable upper limits are derived with respect to that in Run 1. Further results will be released with more data collected in Run 2.

References

1. Phys. Rev. D92, 092004 (2015); 2. ATLAS-CONF-2016-004; 3. ATLAS-CONF-2016-049; 4. ATLAS-CONF-2016-071.